Journal of Gerontology: BIOLOGICAL SCIENCES
2007, Vol. 62A, No. 9, 932–942

Reduction in Glutathione Peroxidase 4 Increases Life Span Through Increased Sensitivity to Apoptosis

Qitao Ran,[1–3] Hanyu Liang,[1,2] Yuji Ikeno,[1–3] Wenbo Qi,[1,2] Tomas A. Prolla,[4] L. Jackson Roberts II,[5] Norman Wolf,[6] Holly VanRemmen,[1–3] and Arlan Richardson[1–3]

[1]Department of Cellular and Structural Biology, and [2]Barshop Institute for Longevity and Aging Studies, the University of Texas Health Science Center at San Antonio.
[3]Geriatric Research, Education and Clinical Center, South Texas Veterans Health Care System, San Antonio.
[4]Departments of Genetics & Medical Genetics, University of Wisconsin-Madison.
[5]Departments of Pharmacology and Medicine, Vanderbilt University, Nashville, Tennessee.
[6]Department of Pathology, University of Washington, Seattle.

Glutathione peroxidase 4 (Gpx4) is an antioxidant defense enzyme that plays an important role in detoxification of oxidative damage to membrane lipids. Because oxidative stress is proposed to play a causal role in aging, we compared the life spans of Gpx4 heterozygous knockout mice (*Gpx4*$^{+/-}$ mice) and wild-type mice (WT mice). To our surprise, the median life span of *Gpx4*$^{+/-}$ mice (1029 days) was significantly longer than that of WT mice (963 days) even though the expression of Gpx4 was reduced approximately 50% in all tissues of *Gpx4*$^{+/-}$ mice. Pathological analysis revealed that *Gpx4*$^{+/-}$ mice showed a delayed occurrence of fatal tumor lymphoma and a reduced severity of glomerulonephritis. Compared to WT mice, *Gpx4*$^{+/-}$ mice showed significantly increased sensitivity to oxidative stress-induced apoptosis. Our data indicate that lifelong reduction in Gpx4 increased life span and reduced/retarded age-related pathology most likely through alterations in sensitivity of tissues to apoptosis.

REACTIVE oxygen species (ROS), such as superoxide and hydrogen peroxide, are constantly generated in aerobic organisms by a variety of pathways; however, the major source of the production of ROS is mitochondria. Although ROS at physiological concentrations may be essential for normal cellular functions, such as cell signaling, excessive amounts of ROS can be detrimental because ROS can cause oxidative damage to lipids, protein, and DNA. Due to the presence of allylic hydrogens, polyunsaturated fatty acids, which are found predominantly in membranes of cells other than adipocytes, are especially vulnerable to attack by ROS (1). The resultant lipid hydroperoxides can be detrimental to cells in two ways. First, lipid hydroperoxides can impair membrane fluidity and function of membrane proteins, which could compromise the function of cells. Second, lipid hydroperoxides can undergo iron- and oxygen-mediated chain-breaking lipid peroxidation to generate reactive aldehydes such as 4-hydroxynonenal (4-HNE) and malondialdehyde (MDA) (2), which can attack other cellular targets, such as proteins and DNA, thereby propagating the initial damage in cellular membranes to other macromolecules and to other parts of cells. Therefore, lipid peroxidation appears to be a primary mechanism in the injury and demise of cells in response to oxidative stress.

The glutathione peroxidases (Gpxs) are a group of selenoproteins that catalyze the reduction of peroxides generated by ROS at the expense of glutathione (3). Four selenium-containing Gpxs have been identified. Gpx1 is the most abundant Gpx and is ubiquitously expressed. Gpx2 is expressed in the gastrointestinal tract. Gpx3 is a plasma form of Gpx. Gpx4, known as phospholipid hydroperoxide glutathione peroxidase, is ubiquitously expressed and is a key enzyme in the detoxification of lipid hydroperoxides (2). All Gpxs can reduce hydrogen peroxide, alkyl peroxides, and fatty acid hydroperoxides; however, Gpx4 also reduces hydroperoxides in lipoproteins and complex lipids such as those derived from cholesterol, cholesteryl esters, and phospholipids. Although Gpx4 is a ubiquitously expressed enzyme, its activity makes up only a small fraction of total cellular Gpx activity in somatic tissues (3). Because of its small size and large hydrophobic surface, Gpx4 can interact with complex lipids in membranes and thereby detoxify membrane lipid hydroperoxides (4). The other major pathway for removing lipid peroxides from membranes is through the coupled actions of phospholipase A_2 (PLA_2) and Gpx1 (5): PLA_2 first excises the fatty acid hydroperoxide from phospholipid hydroperoxide in the membrane, and Gpx1 then reduces the fatty acid hydroperoxide to alcohol and water. Based on kinetic modeling, Gpx4 is estimated to be much more efficient at removing phospholipid hydroperoxides than the PLA_2–Gpx1 pathway because the affinity of Gpx4 to membrane phospholipid hydroperoxides is more than 10^4-fold greater than that of PLA_2 (6). Thus, Gpx4 is considered the primary enzymatic defense system against oxidative damage to cellular membranes (3). Indeed, studies using mice deficient in Gpx4 and transgenic mice overexpressing Gpx4 have shown that Gpx4 is an essential enzyme and plays a critical role in antioxidant defense. For example, the homozygous null mutation of *Gpx4* in mice is embryonic lethal (7,8), and cells

from heterozygous Gpx4 knockout mice show increased lipid peroxidation and more cell death after exposure to oxidizing agents (9). Transgenic mice overexpressing Gpx4 are more resistant to oxidative insults (10), and cortical neurons from Gpx4 transgenic mice are more resistant to β-amyloid cytotoxicity (11). In addition, Gpx4 has been shown to play an important role in regulating apoptosis, and the attributed mechanism appears to be Gpx4's activity in regulating the oxidation of cardiolipin (CL), a mitochondrial membrane lipid that is rich in polyunsaturated fatty acids (12).

One of the most popular theories of aging is the Free Radical or Oxidative Stress Theory of Aging. The basis of this theory is that cells exist in a chronic state of oxidative stress resulting from an imbalance between pro-oxidants and antioxidants. Because of this imbalance, which occurs as a consequence of aerobic metabolism, an accumulation of oxidative damage is proposed to occur with age in a variety of macromolecules within the cell. This steady-state accumulation of oxidative damage is thought to be an important mechanism underlying aging, age-related increases in pathology, and the progressive decline in the functional efficiency of various cellular processes (13,14). Among the macromolecules, polyunsaturated fatty acids in lipids and lipoproteins are the most prone to oxidative damage; therefore, membrane lipid peroxidation is believed to be especially pivotal in aging (15,16). The critical role of lipid peroxidation in aging is supported by studies showing increased levels of lipid peroxidation in aged animals (17,18), as well as by studies showing that calorie restriction, a manipulation known to retard aging, attenuates the age-related increase in lipid peroxidation (17,19). However, whether the modulation of membrane oxidation has a direct effect on life span is not known. Because of the high specificity and efficiency of Gpx4 in removing lipid hydroperoxides from membranes, animal models with altered levels of Gpx4 are expected to show altered levels of lipid peroxidation and, based on the Oxidative Stress Theory of Aging, to show altered aging and/or life spans. We have shown previously that Gpx4 heterozygous knockout (*Gpx4*$^{+/-}$) mice have about a 50% reduction in Gpx4 levels in all tissues, which is consistent with a gene-dosage effect (7). Therefore, the *Gpx4*$^{+/-}$ mouse appears to be an ideal model to test directly the effect of increased membrane lipid peroxidation on aging. If lipid peroxidation plays an essential role in aging, one would predict that *Gpx4*$^{+/-}$ mice, which are more prone to lipid peroxidation of membranes, will have a shortened life span. In this study, we compared the life spans and age-related pathologies between *Gpx4*$^{+/-}$ mice and wild-type (WT) mice. Our results demonstrate that *Gpx4*$^{+/-}$ mice did not have a shortened life span compared to WT mice. In fact, *Gpx4*$^{+/-}$ mice had an increased median survival, and age-related pathology was retarded or reduced in the *Gpx4*$^{+/-}$ mice.

Methods

Animals

Gpx4$^{+/-}$ mice, heterozygous for a targeted mutation in the *Gpx4* gene, were originally generated in the 129 background (7). The mice used in this study were backcrossed 10 times to C57BL/6 mice. All procedures were approved by the Institutional Animal Care and Usage Committee at the University of Texas Health Science Center at San Antonio and the South Texas Veterans Health Care System, Audie L. Murphy Division. The colony of *Gpx4*$^{+/-}$ mice used for this study was generated by breeding male *Gpx4*$^{+/-}$ mice to female WT C57BL/6 mice purchased from The Jackson Laboratory (Bar Harbor, ME). The mice were genotyped at 4–5 weeks of age by polymerase chain reaction (PCR) analysis of DNA obtained from tail clips as previously described (7). The mice were maintained under barrier conditions in a temperature-controlled environment. For the life-span studies, 50 male WT and 50 male *Gpx4*$^{+/-}$ mice born between January 2003 and February 2003 were housed four animals per cage starting at 2 months of age, and were fed a commercial mouse chow (Teklad Diet LM485; Harlan Teklad, Madison, WI) ad libitum. Mice assigned to survival groups were allowed to live out their life span. In other words, there was no censoring in either the WT or the *Gpx4*$^{+/-}$ mice when measuring survival. Life spans for *Gpx4*$^{+/-}$ mice and WT mice were determined by recording the age of spontaneous death of male *Gpx4*$^{+/-}$ and WT mice. The mean, median, 10% (the mean life span of longest-lived 10% animals), and maximum (the age of death for the longest-lived mouse in the cohort) life spans were calculated from the survival data for each genotype.

Cataract Assessment

To assess cataract formation, cataracts were read using a handheld slit lamp at a 30° angle after dilation with 1% tropicamide. Both eyes were scored on an opacity scale of 0, 1, 2, 3, or 4, with 4 representing complete lens opacity as described previously (20).

Measurement of Gpx4 Protein Level and Oxidative Damage

Tissues were collected from male mice and frozen immediately in liquid nitrogen. The tissues were stored at –80°C until used to measure enzyme activities or level of oxidative damage. Levels of Gpx4, Gpx1, catalase, manganese superoxide dismutase (MnSOD), copper/zinc superoxide dismutase (Cu/ZnSOD) were determined as previously described (10).

Plasma and liver levels of F_2-isoprostanes were determined as described by Morrow and Roberts (21). Briefly, blood was collected from the inferior vena cava of anesthetized animals, and then the liver was removed and immediately frozen in liquid nitrogen for storage at –80°C. F_2-isoprostanes were extracted and quantified by gas chromatography-mass spectrometry (GC-MS) using the internal standard, 8-iso Prostaglandin $F_{2\alpha}$-d4 (Cayman Chemical, Ann Arbor, MI), which was added to the samples at the beginning of extraction to correct the yield of the extraction process. The amount of F_2-isoprostanes in liver was expressed as picograms of 8-Iso-$PGF_{2\alpha}$ per milligram of total liver protein, and the amount of F_2-isoprostanes in plasma was expressed as picograms of 8-Iso-$PGF_{2\alpha}$ per milliliter of plasma.

F_4-neuroprostanes in cerebral cortexes, which were dissected out and immediately frozen in liquid nitrogen, were extracted and determined as described by Roberts and colleagues (22). Briefly, after separation by thin layer chromatography, F_4-neuroprostanes were quantified by GC/MS. The amount of F_4-neuroprostanes in brain was expressed as nanograms per gram of total brain protein.

Pathological Analysis

All 50 *Gpx4*$^{+/-}$ mice in the survival group were subjected to end-of-life pathological analysis. We were unable to analyze three of the animals in the WT survival cohort because autolysis was too severe to obtain pathological data; therefore, 47 WT mice were subjected to end-of-life pathological analysis.

After spontaneous death, mice were necropsied for gross pathological lesions. Organs and tissues were excised and preserved in 10% buffered formalin. The fixed tissues were processed conventionally, embedded in paraffin, sectioned at 5 μm, and stained with hematoxylin–eosin. For each mouse, a list of pathological lesions was constructed that included both neoplastic and nonneoplastic diseases. Based on these histopathological data, the tumor burden, disease burden, and severity of each lesion in each mouse were assessed (23). The severity of neoplastic and nephrologic lesions was assessed using the grading system previously described (24,25). For example, glomerulonephritis was graded in order of increasing severity: Grade 0: no lesions; Grade 1: minimal change in glomeruli (minimal glomerulosclerosis); Grade 2: Grade 1 with a few (< 10) casts in renal tubules; Grade 3: Grade 1 with > 10 casts in renal tubules; and Grade 4: Grade 3 with interstitial fibrosis. The probable cause of death for each mouse was determined by the severity of diseases found by necropsy. For neoplastic diseases, cases that had Grade 3 or 4 lesions were categorized as death by neoplastic lesions. For nonneoplastic diseases, cases that had a severe lesion, e.g., Grade 4, associated with other histopathological changes (pleural effusion, ascites, congestion and edema in lung) were categorized as death by nonneoplastic lesions. In $> 90\%$ of the cases, there was agreement by two pathologists. In cases in which there was not agreement or in which no one disease was considered severe enough, the cause of death was evaluated as undetermined.

Measurement of Apoptosis

Male mice, age 26–29 months, received an intraperitoneal injection of diquat dissolved in saline at a dose of 50 mg/kg. This dose is nonlethal, i.e., all of the mice survived this dose of diquat. Six hours after injection, the livers were collected for use in the assays described below. A small piece of liver tissue was fixed in 10% buffered formalin and was embedded in paraffin for the measurement of liver apoptosis. Another piece of liver tissue was homogenized in ice-old buffer I (250 mM mannitol, 75 mM sucrose, 500 μM EGTA, 100 μM EDTA, and 10 mM HEPES, pH 7.4) supplemented with a protease inhibitor cocktail. The homogenates were centrifuged at $600 \times g$ for 10 minutes at 4°C to pellet nuclei and unbroken cells. The resultant supernatant was then centrifuged at $10{,}000 \times g$ for 15 minutes at 4°C to obtain the mitochondrial pellet. The supernatant was further centrifuged at $100{,}000 \times g$ for 60 minutes at 4°C to yield the cytosol. The mitochondrial pellets were washed once in buffer I containing 0.2% (wt/vol) bovine serum albumin (BSA) and twice in buffer I without BSA. The mitochondrial pellets obtained were used for CL peroxidation. The cytosols obtained were used to measure cytochrome *c (cyt. c)* release.

Apoptotic cell counts in the liver were determined in situ by the presence of double-strand DNA breaks observed in paraffin-embedded tissue sections using an in situ oligo ligation (ISOL) kit (Chemicon International, Temecula, CA) with oligo B, according to the manufacturer's instructions. Compared to a conventional TdT-mediated dUTP nick-end labeling (TUNEL) assay, the ISOL assay uses a hairpin oligonucleotide probe to detect more specific DNA fragmentation caused by apoptosis, avoiding randomly damaged DNA (26). Slides were visualized under light microscopy, and the number of positive cells was determined in 10 random fields at ×400 magnification for each liver. Data are expressed as the mean of the ratio of the number of positive cells to the total number of cells in all 10 random fields.

Release of *cyt. c* from mitochondria was detected by measuring the levels of *cyt. c* in cytosol of liver using Western blots. Briefly, cytosolic proteins were separated by sodium dodecyl sulfate–polyacrylamide gel electrophoresis (SDS–PAGE) as described above, and the levels of *cyt. c* were detected using an anti-*cyt. c* antibody (sc-13560; Santa Cruz Biotechnology, Santa Cruz, CA). The intensities of the bands on the blot were quantified with ImageQuant 5.0 (Molecular Dynamics, Sunnyvale, CA) and normalized to a cytosolic loading control (IκB-α) as we have described previously (10).

CL peroxidation was measured by 10-*N*-nonyl-Acridine Orange (NAO; Molecular Probes, Eugene, OR) binding to mitochondria as previously described by Petit and colleagues (27), with modifications. To avoid any potential effect of mitochondrial membrane potential on NAO binding (28), mitochondria were not energized with substrates in these experiments. Briefly, freshly isolated liver mitochondria were resuspended in buffer A (125 mM KCl, 10 mM HEPES, 5 mM $MgCl_2$, and 2 mM K_2HPO_4, pH 7.4). The mitochondrial protein concentration was determined by the Bradford method. An equal amount of mitochondria (10 μg of mitochondrial protein) was added to 200 μL of 20 μM NAO, incubated for 5 minutes, then centrifuged at $30{,}000 \times g$ for 5 minutes. Free dye in the supernatant was determined by measuring absorbance at 495 nm, and the NAO bound to the mitochondria was calculated as the total NAO minus free NAO.

Results

Based on the Oxidative Stress Theory of Aging and the known function of Gpx4 in the protection of cells against oxidative damage, we predicted that a reduced level of Gpx4 would lead to accelerated aging, as shown by a shortened life span. To test if this prediction was valid, we compared

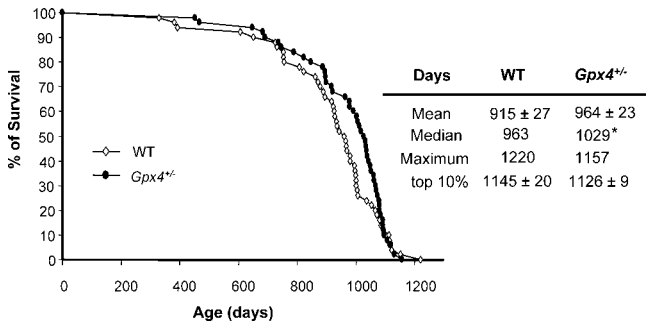

Figure 1. Life span of wild-type (WT) mice and glutathione peroxidase 4 heterozygous knockout (*Gpx4*$^{+/-}$) mice. Kaplan–Meier survival curves are shown for 50 WT (*open diamond*) and 50 *Gpx4*$^{+/-}$ (*solid circle*) mice. The mean (± standard error of the mean [*SEM*]), median, maximum, and top 10% (± *SEM*) survival of male WT and *Gpx4*$^{+/-}$ mice were determined from the age at death as described in the Methods section. *$p < .05$, as determined by median two-sample test.

life spans of *Gpx4*$^{+/-}$ and WT mice. As shown in Figure 1, the life span of *Gpx4*$^{+/-}$ mice was not reduced compared to that of WT mice. In fact, *Gpx4*$^{+/-}$ mice had an increased life span. Compared to that of WT mice, the median life span of *Gpx4*$^{+/-}$ mice was increased by 7%, from 963 days to 1029 days, and this increase is statistically significant. The mean life span of *Gpx4*$^{+/-}$ mice also was longer, about 5% longer than the mean life span of WT mice; however, this difference did not reach statistical significance. The survival curves for these two groups of mice came together at around 1100 days of age, and no difference in mean life span of the top 10% longest-lived animals was observed. The age-dependent mortality rates for *Gpx4*$^{+/-}$ mice and WT mice, as determined by mathematical models described by Pletcher and colleagues (29), were not significantly different (data not shown).

We also compared body weights of *Gpx4*$^{+/-}$ mice and WT mice because it is well established that reduced food consumption, which is shown by reduced body weight, leads to increased life span. As shown in Figure 2A, there was no difference in body weight between *Gpx4*$^{+/-}$ and WT mice from 8 weeks of age up to 24 months of age. Thus, there is no evidence that the *Gpx4*$^{+/-}$ mice are living longer because of reduced caloric intake. Interestingly, the *Gpx4*$^{+/-}$ mice showed less of a decrease in body weight than WT mice starting at 24 months of age, suggesting that the loss in body weight, which is common in aging, was retarded in the *Gpx4*$^{+/-}$ mice.

To determine whether other parameters that change with age are altered in the *Gpx4*$^{+/-}$ mice, the appearance of cataracts in WT and *Gpx4*$^{+/-}$ mice at 25 months of age was determined because the development of cataracts is often used as a biological marker of aging (20). As shown in Figure 2B, there was no difference in cataract development between WT and *Gpx4*$^{+/-}$ mice.

In our previous study (7), we demonstrated that the expression of Gpx4 (messenger RNA and protein) was reduced approximately 50% in 4- to 6-month-old *Gpx4*$^{+/-}$ mice, in comparison to age-matched WT mice. However, we were concerned that the lack of predicted effect on survival of *Gpx4*$^{+/-}$ mice might be due to an up-regulation of the wild-type allele of *Gpx4* gene in older *Gpx4*$^{+/-}$ mice. In other words, the *Gpx4*$^{+/-}$ mice might not be deficient in Gpx4 as they aged. To determine if this is true, we measured Gpx4 protein levels in old *Gpx4*$^{+/-}$ mice and WT mice. As shown in Figure 3, the levels of Gpx4 protein in tissues from 26- to 29-month-old *Gpx4*$^{+/-}$ mice were reduced by approximately 50%, which is similar to what we had observed in young *Gpx4*$^{+/-}$ mice (7). Therefore, the *Gpx4*$^{+/-}$ mice have reduced expression of Gpx4 throughout their life span. Although our previous study found no differences in

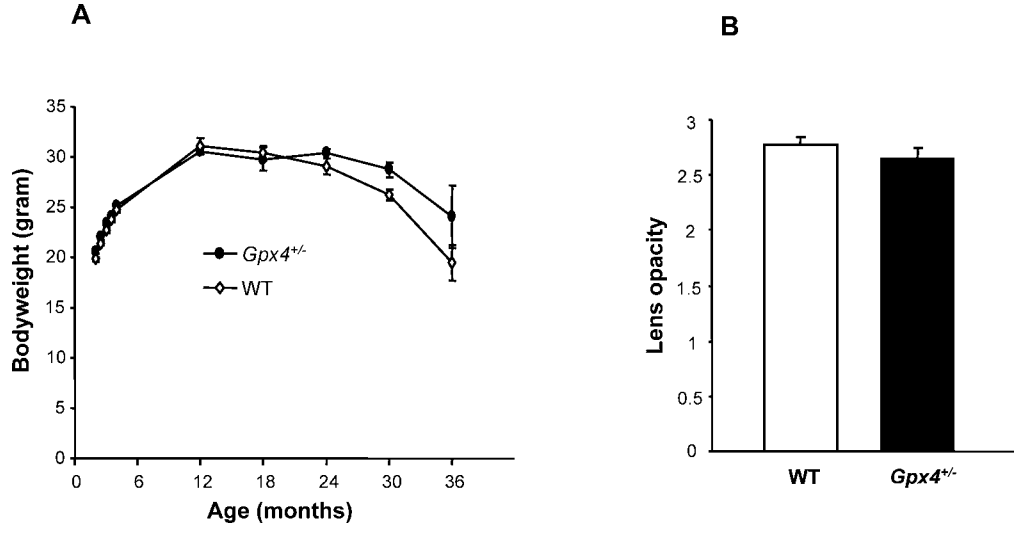

Figure 2. Body weights and cataracts of wild-type (WT) mice and glutathione peroxidase 4 heterozygous knockout (*Gpx4*$^{+/-}$) mice. **A,** Body weights of 12 WT and 12 *Gpx4*$^{+/-}$ mice were determined at indicated intervals throughout their lives. Data are expressed as mean ± standard error of the mean (*SEM*). The difference in the rates of weight loss between WT and *Gpx4*$^{+/-}$ mice is statistically significant ($p = .001$, as determined by mixed-effect linear model). **B,** Cataract formation was assessed in WT and *Gpx4*$^{+/-}$ mice as described in the Methods section. Data are expressed as mean (± *SEM*) for 33 WT mice and 33 *Gpx4*$^{+/-}$ mice.

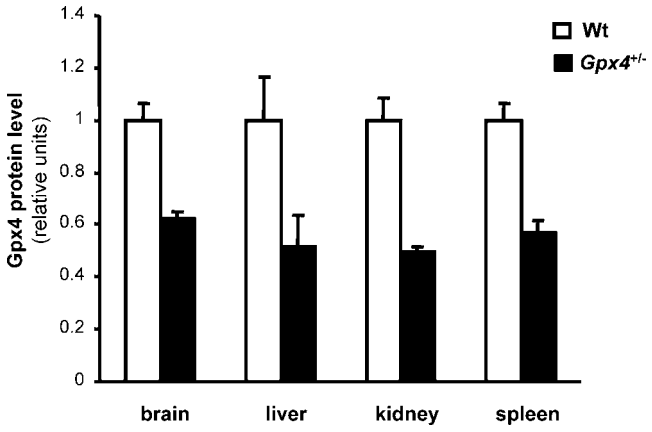

Figure 3. Levels of glutathione peroxidase 4 (Gpx4) in old wild-type (WT) mice and $Gpx4^{+/-}$ mice. Levels of Gpx4 protein in various tissues of 26- to 29-month-old WT and $Gpx4^{+/-}$ mice were determined by Western blots as described in the Methods section. Data are expressed as mean ± standard error of the mean of data obtained from four mice of each genotype. The differences between WT and $Gpx4^{+/-}$ mice are statistically significant for all tissues ($p < .05$, as determined by the Student t test).

other major antioxidant defense enzymes in young $Gpx4^{+/-}$ mice, we were also concerned that the compensatory up-regulation of other antioxidant defense enzymes with age might neutralize the effect of Gpx4 deficiency on survival in $Gpx4^{+/-}$ mice. Thus, we measured levels of other major antioxidant defense enzymes such as Gpx1, MnSOD, and Cu/ZnSOD in old $Gpx4^{+/-}$ and WT mice and found no significant differences in these enzymes between the $Gpx4^{+/-}$ and WT mice (data not shown). Therefore, there was no compensatory up-regulation of other major antioxidant defense enzymes.

To determine whether the reduced Gpx4 level in $Gpx4^{+/-}$ mice led to increased oxidative damage, we compared the levels of lipid peroxidation in old $Gpx4^{+/-}$ and WT mice. Isoprostanes and neuroprostanes are groups of prostaglandin-like compounds that arise from free radical attack on membrane phospholipids. Quantification of F_2-isoprostanes has emerged as an accurate measurement of lipid peroxidation in vivo (30), and we showed that the level of F_2-isoprostanes increases with age in plasma and other tissues of rats and is reduced by caloric restriction (31). Figure 4, A and B, shows the levels F_2-isoprostanes in plasma and liver of $Gpx4^{+/-}$ mice and WT mice. Although the levels of F_2-isoprostane were slightly higher in old $Gpx4^{+/-}$ mice than in old WT mice, the differences were not significant. We also observed no statistically significant difference in DNA oxidation in liver tissue between $Gpx4^{+/-}$ mice and WT mice (data not shown). We also measured the levels F_4-neuroprostane in the brains of $Gpx4^{+/-}$ and WT mice. F_4-neuroprostanes are derived from oxidized docosahexaenoic acid, whereas F_2-isoprostanes are derived from oxidized arachidonic acid. Docosahexaenoic acid is more prone to oxidation than arachidonic acid and is highly enriched in brain (22). We observed a 52% increase in F_4-neuroprostanes levels in brains of old $Gpx4^{+/-}$ mice over old WT mice, and this increase is statistically significant.

To determine whether the increase in the life span of the $Gpx4^{+/-}$ mice was related to changes in the incidence of pathological lesions, we conducted a comprehensive pathological analysis on the mice in the survival groups after they died. As shown in Table 1, the probable causes of death for the WT and $Gpx4^{+/-}$ mice were similar: Approximately 55%–60% of the WT and $Gpx4^{+/-}$ mice died of neoplastic diseases, and the $Gpx4^{+/-}$ mice showed no reduction in occurrence of fatal tumors compared to WT mice. As expected for mice in the C57BL/6 background, the majority of fatal tumors in both WT and $Gpx4^{+/-}$ mice was lymphoma. Interestingly, the $Gpx4^{+/-}$ mice that died from lymphoma had a longer median age than the WT mice that died from lymphoma (963 days vs 928 days). In addition, whereas 37.5% of $Gpx4^{+/-}$ mice that died from lymphoma

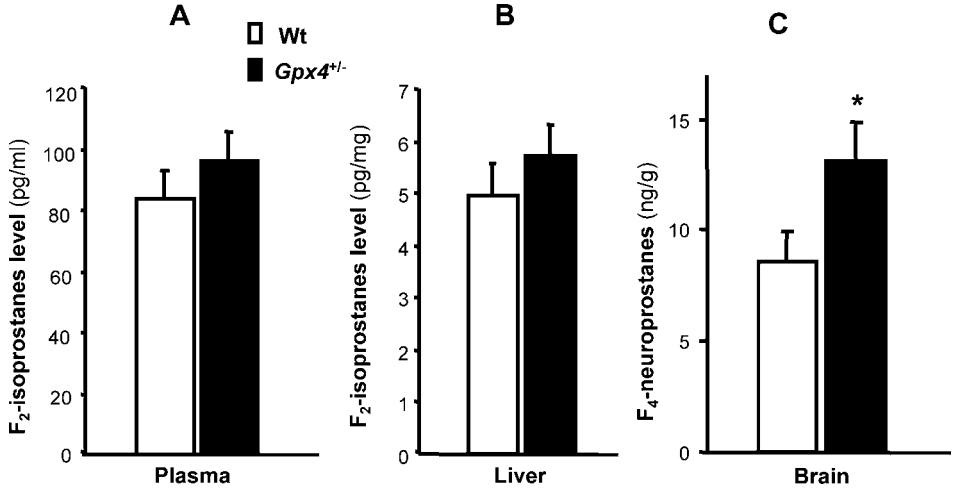

Figure 4. Levels of lipid peroxidation WT and glutathione peroxidase 4 heterozygous knockout ($Gpx4^{+/-}$) mice. Levels of F_2-isoprostanes in the plasma (**A**) and liver (**B**), and F_4-neuroprostanes in brain (**C**) of 26- to 29-month-old WT and $Gpx4^{+/-}$ mice were determined as described in the Methods section. Data are expressed as mean ± standard error of the mean for four mice of each genotype (*$p < .05$, as determined by Student's t test).

Table 1. End-of-Life Pathology for WT and *Gpx4*$^{+/-}$ Mice

	WT	*Gpx4*$^{+/-}$
Neoplasm	26	30
Lymphoma	18	24
Others	8	6
Nonneoplasm	14	12
Glomerulonephritis	10*	0
AMP	3	10
Others	1	2
Undetermined	7	8
Total	47	50

Notes: The numbers of fatal neoplasm and fatal nonneoplasm in glutathione peroxidase 4 heterozygous knockout (*Gpx4*$^{+/-}$) mice ($n = 50$) and in wild type (WT) mice ($n = 47$) in the survival groups were determined as described in the Methods section. AMP, acidophilic macrophage pneumonia.

*$p < .01$, as determined by Fisher's exact test.

were older than 1026 days, only 16.7% of WT mice that died from lymphoma died at ages above 1026 days. To determine whether the incidence of death from lymphoma in the survival groups were different as a function of age, we followed the incidence of death when the majority of mice began to die, i.e., after 900 days of age, when the difference in survival is greatest. As shown in Figure 5A, the age of this group of *Gpx4*$^{+/-}$ mice is higher than the age of the group of WT mice, indicating that the occurrence of fatal lymphoma was delayed in *Gpx4*$^{+/-}$ mice.

The major nonneoplastic pathology observed in WT and *Gpx4*$^{+/-}$ mice was glomerulonephritis. About 20% of WT mice in the survival group died of glomerulonephritis, whereas none of the *Gpx4*$^{+/-}$ mice in the survival group died of glomerulonephritis. To determine whether the reduced deaths from glomerulonephritis in the *Gpx4*$^{+/-}$ mice occurred because of changes in the initiation and/or development/progression of the disease, we compared the total incidence and severity of glomerulonephritis in mice in the survival groups. Our data indicated that 42 (of 47) WT mice and 47 (of 50) *Gpx4*$^{+/-}$ mice had glomerulonephritis, indicating that the total incidence of glomerulonephritis was similar for *Gpx4*$^{+/-}$ mice and WT mice. However, as shown in Figure 5B, the severity of glomerulonephritis was significantly reduced in *Gpx4*$^{+/-}$ mice. Therefore, it appears that the progression/development of glomerulonephritis was suppressed in *Gpx4*$^{+/-}$ mice. The data in Table 1 also show that death from acidophilic macrophage pneumonia (AMP) was higher for the *Gpx4*$^{+/-}$ mice than for the WT mice, but that the difference between the two groups is not statically significant. Interestingly, 90% of the deaths from AMP occurred late in the life span of the *Gpx4*$^{+/-}$ mice (after 1044 days of age) and where the survival curves of the *Gpx4*$^{+/-}$ and WT mice are shown to merge. Thus, the lack of an increase in the maximum survival of the *Gpx4*$^{+/-}$ mice could be due to a greater propensity of the old *Gpx4*$^{+/-}$ mice to die from AMP.

Increased apoptosis could remove damaged cells that could otherwise give rise to increased cancer or pathology (32). Because Gpx4 is shown to play an important role in regulating apoptosis (12), it is possible that the delayed occurrence of fatal lymphoma and reduced severity of glomerulonephritis were due to altered apoptosis in tissues of *Gpx4*$^{+/-}$ mice. Therefore, we compared the induction of apoptosis by oxidative stress in old *Gpx4*$^{+/-}$ mice and WT mice when differences in survival and pathology were observed. When injected intraperitoneally, diquat, a superoxide generator, affects primarily liver (33). As shown in Figure 6A, apoptotic cell levels were low in untreated animals, and no difference in levels of apoptotic cells was observed in untreated old *Gpx4*$^{+/-}$ mice and WT mice. However, after diquat treatment, *Gpx4*$^{+/-}$ mice had significantly more apoptotic cells than their WT counterparts had, indicating that old *Gpx4*$^{+/-}$ mice were more

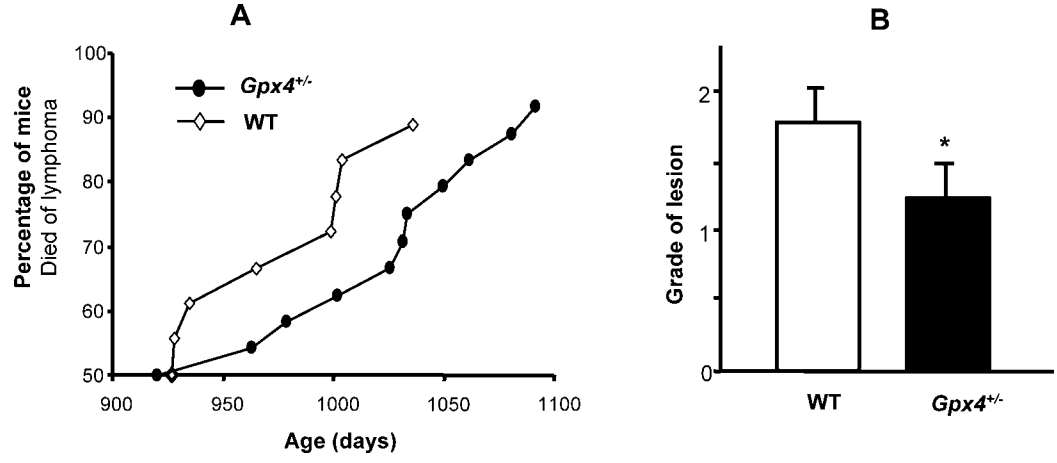

Figure 5. Age related pathology in wild-type (WT) mice and glutathione peroxidase 4 heterozygous knockout (*Gpx4*$^{+/-}$) mice. **A,** Percentage of mice dying from fatal lymphoma (WT and *Gpx4*$^{+/-}$) between 920 and 1092 days of age, when the difference in the survival of WT and *Gpx4*$^{+/-}$ mice was greatest. The age difference between *Gpx4*$^{+/-}$ mice and WT mice is statistically significant as determined by log-rank test ($p < .05$). **B,** Severity of glomerulonephritis at end of life in WT and *Gpx4*$^{+/-}$ mice was determined as described in the Methods section. Data are expressed as mean ± standard error of the mean for 50 WT mice and 47 *Gpx4*$^{+/-}$ mice (*$p < .05$, as determined by Student's t test).

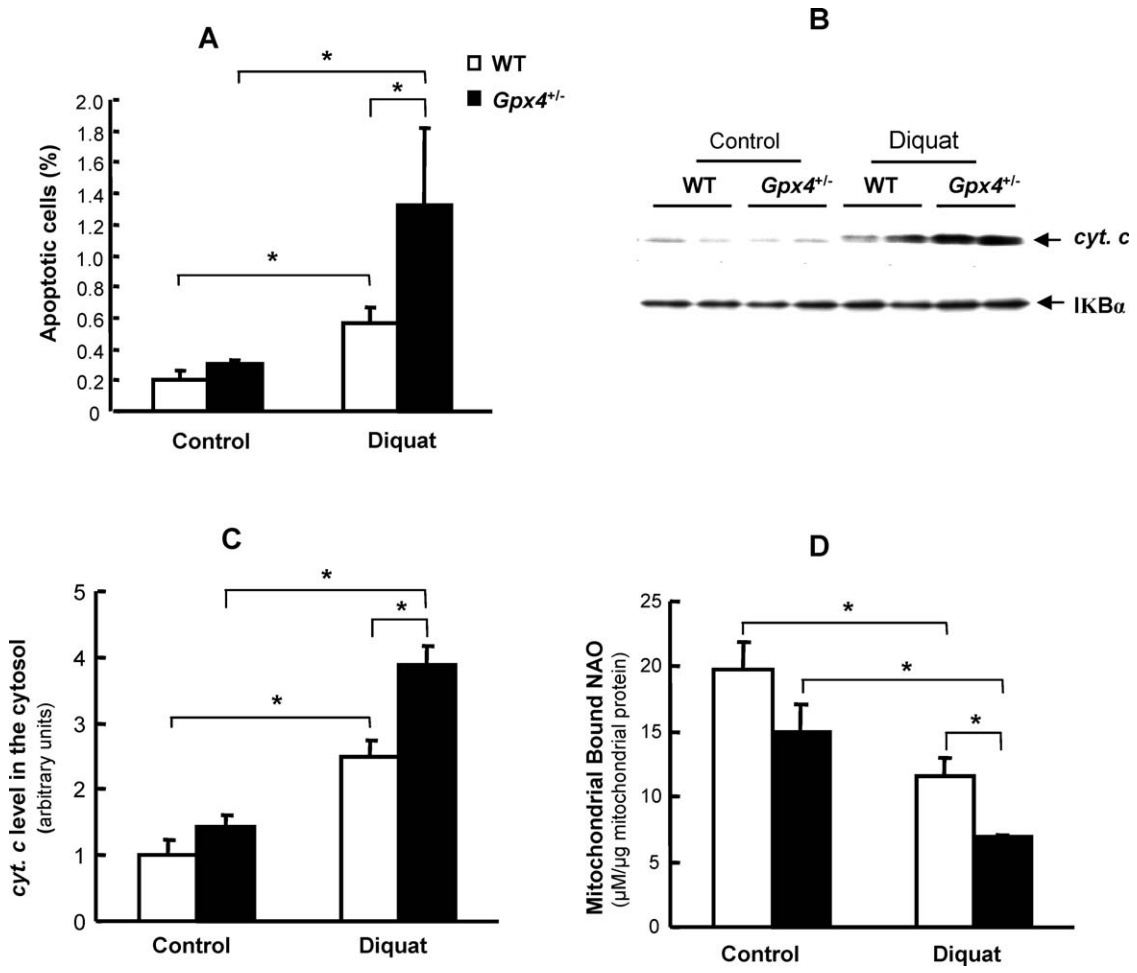

Figure 6. Apoptosis in old wild-type (WT) mice and glutathione peroxidase 4 heterozygous knockout ($Gpx4^{+/-}$) mice. Mice that were 26–29 months of age were treated with diquat (50 mg/kg) for 6 hours, and the following parameters were measured in the livers of WT (*open bars*) and $Gpx4^{+/-}$ (*solid bars*), as described in the Methods section. **A,** Level of apoptosis before (control) and after diquat treatment. **B,** Photograph of a representative Western blot showing cytochrome *c* (*cyt. c*) release into the cytosol. **C,** Quantification of *cyt. c* release as determined from Western blots before (control) and after diquat treatment. **D,** Cardiolipin peroxidation as measured by mitochondrial bound NAO before (control) and after diquat treatment. All values are expressed as mean ± standard error of the mean of data obtained from four mice. $*p < .05$ level.

sensitive to diquat-induced apoptosis. Release of *cyt. c* from the mitochondria is a critical early event in the initiation of the intrinsic pathway (mitochondrial pathway) of apoptosis (34), and studies show that Gpx4 can regulate the intrinsic pathway of apoptosis by altering *cyt. c* release from mitochondria (10,35). Therefore, we also compared cytosolic *cyt. c* levels in livers from old $Gpx4^{+/-}$ and WT mice (Figure 6B). As shown in Figure 6C, without treatment, there was no statistically significant difference in cytosolic levels of *cyt. c* between $Gpx4^{+/-}$ mice and WT mice. Diquat treatment resulted in an increase in cytosolic *cyt. c* levels in both $Gpx4^{+/-}$ mice and WT; however, cytosolic levels of *cyt. c* were significantly higher in livers of $Gpx4^{+/-}$ mice than in livers of WT mice, indicating increased release of *cyt. c* from mitochondria in $Gpx4^{+/-}$ mice.

To determine the mechanism underlying the effect of Gpx4 deficiency on the induction of apoptosis by oxidative stress, we measured CL oxidation. CL is a phospholipid that localizes exclusively in mitochondria, primarily the inner membrane, and binds to c*yt. c*. Due to its high content of polyunsaturated fatty acids, CL is easily oxidizable, and peroxidized CL loses its ability to bind to *cyt. c*, leading to *cyt. c* release from mitochondria (36). Gpx4 is shown to rapidly reduce CL hydroperoxide (CLOOH) to its alcohol derivative (CLOH), which can bind *cyt. c* as well as CL, thereby preventing *cyt. c* release from mitochondrial inner membrane (37). To determine whether the level of CL peroxidation was altered in $Gpx4^{+/-}$ mice, we measured levels of CLOOH in $Gpx4^{+/-}$ and WT mice by the NAO binding assay. NAO is a lipophilic dye that has a 30-fold greater affinity for CL over other anionic phospholipids such as phosphatidylserine and phosphatidylinositol, and does not bind phosphatidylcholine and phosphatidylethanolamine (27). NAO has been extensively used for visualization and quantification of CL in isolated mitochondria as well as in living cells (27,38–40). However, a recent study (41)

questioned the specificity of NAO binding to CL in living cells. To avoid any possible interference from other lipid components, we used isolated liver mitochondria because mitochondria have only trace levels of phosphatidylserine and phosphatidylinositol; thus, the observed NAO binding would come from CL. CL peroxidation was measured by the loss of NAO binding to the mitochondria because the fluorochrome has no affinity for CL hydroperoxide (38,42,43). As shown in Figure 6D, NAO binding was reduced in mitochondria from untreated, old *Gpx4*$^{+/-}$ mice compared to old WT mice; however, this decrease was not statistically significant. Diquat treatment resulted in a significant decrease in NAO binding to mitochondria isolated from both *Gpx4*$^{+/-}$ and WT mice, showing an increase in CL peroxidation. However, NAO binding was significantly reduced in the *Gpx4*$^{+/-}$ mice compared to the WT mice, indicating that old *Gpx4*$^{+/-}$ mice had increased levels of CL peroxidation after diquat treatment.

Discussion

According to the popular Oxidative Stress Theory of Aging, the steady-state accumulation of oxidative damage plays an important role in the biological mechanism underlying aging, leading to age-related increases in pathology as well as to progressive declines in the functional efficiency of cells/tissues (13,14). Polyunsaturated fatty acids in lipids and lipoproteins are especially prone to oxidative damage, and an increase in lipid peroxidation is shown to occur with increasing age (17,18). The age-related increase in oxidative damage to membrane lipids could be physiologically important to an organism because lipid peroxidation is shown to play an important role in a variety of cellular processes, e.g., inactivation of membrane enzymes, alterations in functions of ion channels, collapse of membrane potential, and reduced mitochondria functions such as respiration (44).

To study the role of lipid peroxidation to membranes in aging, we used a unique mouse model, *Gpx4*$^{+/-}$ mice, which we recently generated and characterized. Gpx4 is an antioxidant enzyme in the Gpx family. Whereas all Gpxs, including Gpx4, reduce hydrogen peroxide, alkyl peroxides, and fatty acid hydroperoxides, Gpx4 is unique in that it also reduces hydroperoxides in lipoproteins and complex lipids such as those derived from cholesterol, cholesteryl esters, and phospholipids. Therefore, Gpx4 is thought to play a key role in protecting membrane lipids from oxidative damage (3). We showed that knockout mice null for Gpx4 die during early embryonic development and that *Gpx4*$^{+/-}$ mice, which have only one WT allele of the *Gpx4* gene, appear normal but have approximately 50% less Gpx4 in all tissues compared to WT mice. *Gpx4*$^{+/-}$ mice and cells are more sensitive to oxidative stress (9). Because the levels of Gpx1 and catalase, two major antioxidant defense enzymes involved in reducing H_2O_2 and free fatty acid hydroperoxides, are similar in *Gpx4*$^{+/-}$ mice and WT mice (7), and because Gpx1 and catalase are at much higher levels than Gpx4 in all tissue except testes, the cells/tissues of *Gpx4*$^{+/-}$ mice are only deficient in their ability to protect membrane lipids from peroxidation. Therefore, these mice are ideal for studying the role of lipid peroxidation of membranes in aging and other biological processes.

Based on the Oxidative Stress Theory of Aging and the potential physiological importance of membrane lipid peroxidation in cellular functions, we hypothesized that the *Gpx4*$^{+/-}$ mice would show accelerated aging, i.e., reduced life span. In contrast, if lipid peroxidation of membranes plays no role in aging, we would see no difference between the life spans of the *Gpx4*$^{+/-}$ and WT mice. We were surprised when we observed an increase in life span (which was significant for the median life span) in the *Gpx4*$^{+/-}$ mice. One might argue that the 7% increase in median life span, although statistically significant, is not impressive compared to the 15%–30% increase in life span found in studies of other genetically altered mouse models (reviewed in 45). However, it should be noted that the median survival that we observed for the *Gpx4*$^{+/-}$ mice (1029 days or 34.3 months) is extremely long for C57BL/6 mice and is longer than that of many of the long-lived mutant mouse models previously reported, e.g., *Igf1r*$^{+/-}$ mice (median life span of about 25.4 months) (46), FIRKO mice (median life span of 33.4 months) (47), transgenic mice overexpressing catalase in mitochondria (median life span of about 31.0 months) (48), GHR/BP$^{-/-}$ mice (median life span of 31.4 months) (49), *p66*$^{sch-/-}$ mice (median life span of 32.4 months) (50), and Klotho mice (median life span of about 33.2 months) (51). Therefore, we believe that the modest increase in life span of the *Gpx4*$^{+/-}$ mice is important because it results in one of the longest-lived genetic mutant mouse models generated to date.

The life span of *Gpx4*$^{+/-}$ mice appears to be inconsistent with the Oxidative Stress Theory of Aging, i.e., increased oxidative stress should reduce life span, not extend life span. Previously, our group showed that *Sod2*$^{+/-}$ mice, which have reduced expression of MnSOD in all tissues and increased levels of oxidative damage to DNA, had an identical life span as control, WT mice (52). The life-span data of *Gpx4*$^{+/-}$ and *Sod2*$^{+/-}$ mice show that a deficiency in one component of the antioxidant defense does not directly lead to accelerated aging in mice.

The increase in the median survival of *Gpx4*$^{+/-}$ mice was most likely a result of altered pathology. Our pathological analysis of mice in the survival groups revealed two significantly altered pathologies that may contribute to increased median survival of the *Gpx4*$^{+/-}$ mice: delayed occurrence of fatal lymphoma and reduced severity of glomerulonephritis. Lymphoma is a major fatal neoplasm in C57BL/6 mice, the incidence of which increases with age (53). Our pathological data indicate that the age-related increase in occurrence and/or progression of lymphoma was delayed in *Gpx4*$^{+/-}$ mice, i.e., the *Gpx4*$^{+/-}$ mice died of fatal lymphoma at older ages than did the WT mice. We also observed that glomerulonephritis, an age-associated nephropathy, was reduced in *Gpx4*$^{+/-}$ mice. Our data suggested that the reduction in fatal glomerulonephritis in *Gpx4*$^{+/-}$ mice was due to the suppression in the progression/development, but not the initiation, of glomerulonephritis. Hence, does the reduced Gpx4 expression increase life span and retard/reduce pathology by slowing down aging? Even though we observed that reduced expression of Gpx4

delayed the terminal loss of body weight associated with aging (54), our data would tend to indicate that aging is not altered because neither the 10% survival, maximum survival, age-dependent mortality rate nor cataract development was altered in the *Gpx4*$^{+/-}$ mice.

One potential explanation for the improved pathology is an increase in apoptosis that would remove damaged/abnormal cells. Gpx4 appears to play an important role in regulating apoptosis. For example, the overexpression of Gpx4 inhibits the induction of apoptosis by a variety of oxidizing agents (55–57). Additionally, Gpx4 alters apoptosis through the intrinsic pathway by its ability to rapidly reduce hydroperoxides in CL, a mitochondrial inner membrane phospholipid that binds to c*yt. c*. Because of its high content (80%–90%) of linoleic acid (58), CL is vulnerable to free radical oxidation, and peroxidation of CL leads to *cyt. c* release from mitochondria. Using monolayers of CL, Nomura and colleagues (37) showed that oxidation of CL to CLOOH decreased *cyt. c* binding. Gpx4 can rapidly reduce CLOOH to CLOH (37), and the resultant CLOH can bind *cyt. c* as well as nonoxidized CL (37,58,59). In our previous study with Gpx4 transgenic mice exposed to diquat, we showed that liver from mice overexpressing Gpx4 had reduced levels of apoptosis and decreased *cyt. c* release from mitochondria, indicating that Gpx4 also plays an important role in regulating apoptosis in vivo (10). In this study, we showed that diquat treatment induced more apoptotic cells in livers of *Gpx4*$^{+/-}$ mice than in WT mice. In addition, the *Gpx4*$^{+/-}$ mice had increased *cyt. c* release from mitochondria and increased levels of mitochondrial CL peroxidation compared to WT mice after diquat treatment. Therefore, *Gpx4*$^{+/-}$ mice appear to have increased sensitivity to stress-induced apoptosis compared to WT mice.

Increased apoptosis has been proposed to have both beneficial and detrimental effects on aging in mammalian systems (60). On one hand, increased apoptosis in postmitotic cells, such as neurons and cardiomyocytes, could be detrimental. On the other hand, increased apoptosis could serve as an important cellular defense mechanism by maintaining genetic stability through the elimination of damaged and dysfunctional cells (61). Altered sensitivity to apoptosis is known to alter the occurrence of tumors, such as lymphoma (32). Therefore, increased sensitivity to apoptosis likely contributed to the delayed occurrence of fatal lymphoma in *Gpx4*$^{+/-}$ mice. Increased apoptosis also could be beneficial in preventing glomerulonephritis through mechanisms such as the deletion of infiltrating leukocytes and restoration of normal glomerular structure (62). Therefore, at the present time, we believe the most likely explanation for the increased life span of the *Gpx4*$^{+/-}$ mice is through reduced pathology in certain cells/tissues because of increased sensitivity to apoptosis.

Our observations on aging in *Gpx4*$^{+/-}$ mice appear to be in contrast to what has been reported for *p66*$^{shc-/-}$ mice. p66^{shc} is shown to act as an oxidoreductase to generate ROS in mitochondria and activate the mitochondrial pathway of apoptosis by enhancing *cyt. c* release from mitochondria (63). Migliaccio and colleagues (50,64) showed that the life span of *p66*$^{shc-/-}$ mice was increased by 30% over control WT mice, and the increase in life span in *p66*$^{shc-/-}$ mice was correlated with reduced apoptosis in murine embryonic fibroblasts isolated from *p66*$^{shc-/-}$ mice after oxidative stress and increased survival of *p66*$^{shc-/-}$ mice after paraquat injection (50). In contrast, we showed in this study that the median life span of *Gpx4*$^{+/-}$ mice was increased by 7%, and we showed previously that murine embryonic fibroblasts from *Gpx4*$^{+/-}$ mice had increased apoptosis after oxidative stress and that *Gpx4*$^{+/-}$ mice had reduced survival after γ irradiation (7,9). Therefore, increased sensitivity to apoptosis (in *Gpx4*$^{+/-}$ mice) and reduced sensitivity to apoptosis (in *p66*$^{shc-/-}$ mice) are both correlated with increased life spans. As previously noted (60), the role of apoptosis in aging is very complex. The status of reduced or increased apoptosis in different cells and tissues could affect age-related pathology differently. We showed that the occurrence of fatal lymphoma was delayed in *Gpx4*$^{+/-}$ mice and that *Gpx4*$^{+/-}$ mice also had retarded glomerulonephritis. Unfortunately, there were no data on the pathology of the *p66*$^{shc-/-}$ mice in the life-span study (50), so we can not compare age-related pathology between *Gpx4*$^{+/-}$ mice and *p66*$^{shc-/-}$ mice.

Acknowledgments

This study was supported by a Reserve Educational Assistance Program (REAP) and a Merit Award (HVR) from the Department of Veteran Affairs; by National Institutes of Health grants P01 AG19316, P01AG020591, R37GM42056; and by the San Antonio Nathan Shock Aging Center (1P30-AG13319).

We thank Clyde Alex McMahan and John Cornell for help with statistical analysis in this study.

Drs. Ran, Liang, and Ikeno contributed equally to this work.

Correspondence

Address correspondence to Arlan Richardson, PhD, Barshop Institute for Longevity and Aging Studies, 15355 Lambda Drive, San Antonio, TX 78245-3207. E-mail: richardsona@uthscsa.edu

References

1. Porter NA, Caldwell SE, Mills KA. Mechanisms of free radical oxidation of unsaturated lipids. *Lipid.* 1995;30:277–290.
2. Girotti AW. Lipid hydroperoxide generation, turnover, and effector action in biological systems. *J Lipid Res.* 1998;39:1529–1542.
3. Brigelius-Flohe R. Tissue-specific functions of individual glutathione peroxidases. *Free Radic Biol Med.* 1999;27:951–965.
4. Ursini F, Bindoli A. The role of selenium peroxidases in the protection against oxidative damage of membranes. *Chem Phys Lipids.* 1987;44:255–276.
5. van Kuijk FJ, Handelman GJ, Dratz EA. Consecutive action of phospholipase A2 and glutathione peroxidase is required for reduction of phospholipid hydroperoxides and provides a convenient method to determine peroxide values in membranes. *J Free Radic Biol Med.* 1985;1:421–427.
6. Antunes F, Salvador A, Pinto RE. PHGPx and phospholipase A2/GPx: comparative importance on the reduction of hydroperoxides in rat liver mitochondria. *Free Radic Biol Med.* 1995;19:669–677.
7. Yant LJ, Ran Q, Rao L, et al. The selenoprotein GPX4 is essential for mouse development and protects from radiation and oxidative damage insults. *Free Radic Biol Med.* 2003;34:496–502.
8. Imai H, Hirao F, Sakamoto T, et al. Early embryonic lethality caused by targeted disruption of the mouse PHGPx gene. *Biochem Biophys Res Commun.* 2003;305:278–286.
9. Ran Q, Van Remmen H, Gu M, et al. Embryonic fibroblasts from Gpx4+/– mice: a novel model for studying the role of membrane

peroxidation in biological processes. *Free Radic Biol Med.* 2003; 35:1101–1109.
10. Ran Q, Liang H, Gu M, et al. Transgenic mice overexpressing glutathione peroxidase 4 are protected against oxidative stress-induced apoptosis. *J Biol Chem.* 2004;279:55137–55146.
11. Ran Q, Gu M, Van Remmen H, et al. Glutathione peroxidase 4 protects cortical neurons from oxidative injury and amyloid toxicity. *J Neurosci Res.* 2006;84:202–208.
12. Imai H, Nakagawa Y. Biological significance of phospholipid hydroperoxide glutathione peroxidase (PHGPx, GPx4) in mammalian cells. *Free Radic Biol Med.* 2003;34:145–169.
13. Warner HR. Superoxide dismutase, aging, and degenerative disease. *Free Radic Biol Med.* 1994;17:249–258.
14. Bohr VA, Anson RM. DNA damage, mutation and fine structure DNA repair in aging. *Mutat Res.* 1995;338:25–34.
15. Yu BP. Antioxidant action of dietary restriction in aging. *J Nutr Sci Vitaminol.* 1993;39:575–583.
16. Sanz A, Pamplona R, Barja G. Is the mitochondrial free radical theory of aging intact? *Antioxid Redox Signal.* 2006;8:582–599.
17. Laganiere S, Yu BP. Modulation of membrane phospholipid fatty acid composition by age and food restriction. *Gerontology.* 1993;39: 7–18.
18. Lambert AJ, Portero-Otin M, Pamplona R, et al. Effect of ageing and caloric restriction on specific markers of protein oxidative damage and membrane peroxidizability in rat liver mitochondria. *Mech Ageing Dev.* 2004;125:529–538.
19. Pamplona R, Portero-Otin M, Requena J, et al. Oxidative, glycoxidative and lipoxidative damage to rat heart mitochondrial proteins is lower after 4 months of caloric restriction than in age-matched controls. *Mech Ageing Dev.* 2002;123:1437–1446.
20. Wolf NS, Li Y, Pendergrass W, et al. Normal mouse and rat strains as models for age-related cataract and the effect of caloric restriction on its development. *Exp Eye Res.* 2000;70:683–692.
21. Morrow JD, Roberts LJ. Mass spectrometric quantification of F2-isoprostanes in biological fluids and tissues as measure of oxidant stress. *Methods Enzymol.* 1999;300:3–12.
22. Roberts LJ, Montine TJ, Markesbery WR, et al. Formation of isoprostane-like compounds (neuroprostanes) in vivo from docosahexaenoic acid. *J Biol Chem.* 1998;273:13605–13612.
23. Bronson RT, Lipman RD. Reduction in rate of occurrence of age related lesions in dietary restricted laboratory mice. *Growth Dev Aging.* 1991;55:169–184.
24. Ikeno Y, Bronson RT, Hubbard GB, et al. Delayed occurrence of fatal neoplastic diseases in Ames dwarf mice: correlation to extended longevity. *J Gerontol A Biol Sci Med Sci.* 2003;58: 291–296.
25. Ikeno Y, Hubbard GB, Lee S, et al. Housing density does not influence the longevity effect of calorie restriction. *J Gerontol A Biol Sci Med Sci.* 2005;60:1510–1517.
26. Tanaka M, Nakae S, Terry RD, et al. Cardiomyocyte-specific Bcl-2 overexpression attenuates ischemia-reperfusion injury, immune response during acute rejection, and graft coronary artery disease. *Blood.* 2004;104:3789–3796.
27. Petit JM, Maftah A, Ratinaud MH, Julien R. 10N-nonyl acridine orange interacts with cardiolipin and allows the quantification of this phospholipid in isolated mitochondria. *Eur J Biochem.* 1992;209: 267–273.
28. Jacobson J, Duchen MR, Heales SJ. Intracellular distribution of the fluorescent dye nonyl acridine orange responds to the mitochondrial membrane potential: implications for assays of cardiolipin and mitochondrial mass. *J Neurochem.* 2002;82:224–233.
29. Pletcher SD, Khazaeli AA, Curtsinger JW. Why do life spans differ? Partitioning mean longevity differences in terms of age-specific mortality parameters. *J Gerontol Biol Sci Med Sci.* 2000;55A: B381–B389.
30. Roberts LJ, Morrow JD. Isoprostanes. Novel markers of endogenous lipid peroxidation and potential mediators of oxidant injury. *Ann N Y Acad Sci.* 1994;744:237–242.
31. Ward WF, Qi W, Van Remmen H, et al. Effects of age and caloric restriction on lipid peroxidation: measurement of oxidative stress by F2-isoprostane levels. *J Gerontol A Biol Sci Med Sci.* 2005;60: 847–851.
32. Jacks T, Remington L, Williams BO, et al. Tumor spectrum analysis in p53-mutant mice. *Curr Biol.* 1994;4:1–7.
33. Jones GM, Vale JA. Mechanisms of toxicity, clinical features, and management of diquat poisoning: a review. *J Toxicol Clin Toxicol.* 2000;38:123–128.
34. Budihardjo I, Oliver H, Lutter M, et al. Biochemical pathways of caspase activation during apoptosis. *Annu Rev Cell Dev Biol.* 1999;15: 269–290.
35. Nomura K, Imai H, Koumura T, et al. Mitochondrial phospholipid hydroperoxide glutathione peroxidase suppresses apoptosis mediated by a mitochondrial death pathway. *J Biol Chem.* 1999;274: 29294–29302.
36. Kagan VE, Tyurin VA, Jiang J, et al. Cytochrome *c* acts as a cardiolipin oxygenase required for release of proapoptotic factors. *Nat Chem Biol.* 2005;1:223–232.
37. Nomura K, Imai H, Koumura T, et al. Mitochondrial phospholipid hydroperoxide glutathione peroxidase inhibits the release of cytochrome *c* from mitochondria by suppressing the peroxidation of cardiolipin in hypoglycaemia-induced apoptosis. *Biochem J.* 2000; 351(Pt 1):183–193.
38. Garcia Fernandez MI, Ceccarelli D, Muscatello U. Use of the fluorescent dye 10-*N*-nonyl acridine orange in quantitative and location assays of cardiolipin: a study on different experimental models. *Anal Biochem.* 2004;328:174–180.
39. Maftah A, Petit JM, Julien R. Specific interaction of the new fluorescent dye 10-*N*-nonyl acridine orange with inner mitochondrial membrane. A lipid-mediated inhibition of oxidative phosphorylation. *FEBS Lett.* 1990;260:236–240.
40. Luchetti F, Canonico B, Mannello F, et al. Melatonin reduces early changes in intramitochondrial cardiolipin during apoptosis in U937 cell line. *Toxicol In Vitro.* 2007;21:293–301.
41. Gohil VM, Gvozdenovic-Jeremic J, Schlame M, et al. Binding of 10-*N*-nonyl acridine orange to cardiolipin-deficient yeast cells: implications for assay of cardiolipin. *Anal Biochem.* 2005;343:350–352.
42. Kirkinezos IG, Bacman SR, Hernandez D, et al. Cytochrome *c* association with the inner mitochondrial membrane is impaired in the CNS of G93A-SOD1 mice. *J Neurosci.* 2005;25:164–172.
43. Viola G, Salvador A, Vedaldi D, et al. Induction of apoptosis by photoexcited tetracyclic compounds derivatives of benzo[b]thiophenes and pyridines. *J Photochem Photobiol B.* 2006;82:105–116.
44. Stark G. Functional consequences of oxidative membrane damage. *J Membr Biol.* 2005;205:1–16.
45. Liang H, Masoro EJ, Nelson JF, et al. Genetic mouse models of extended lifespan. *Exp Gerontol.* 2003;38:1353–1364.
46. Holzenberger M, Dupont J, Ducos B, et al. IGF-1 receptor regulates lifespan and resistance to oxidative stress in mice. *Nature.* 2003;421: 182–187.
47. Bluher M, Kahn BB, Kahn CR. Extended longevity in mice lacking the insulin receptor in adipose tissue. *Science.* 2003;299:572–574.
48. Schriner SE, Linford NJ, Martin GM, et al. Extension of murine life span by overexpression of catalase targeted to mitochondria. *Science.* 2005;308:1909–1911.
49. Coschigano KT, Holland AN, Riders ME, et al. Deletion, but not antagonism, of the mouse growth hormone receptor results in severely decreased body weights, insulin, and insulin-like growth factor I levels and increased life span. *Endocrinology.* 2003;144: 3799–3810.
50. Migliaccio E, Giorgio M, Mele S, et al. The p66shc adaptor protein controls oxidative stress response and life span in mammals. *Nature.* 1999;402:309–313.
51. Kurosu H, Yamamoto M, Clark JD, et al. Suppression of aging in mice by the hormone Klotho. *Science.* 2005;309:1829–1833.
52. Van Remmen H, Ikeno Y, Hamilton M, et al. Life-long reduction in MnSOD activity results in increased DNA damage and higher incidence of cancer but does not accelerate aging. *Physiol Genomics.* 2003;16:29–37.
53. Haines DC, Chattopadhyay S, Ward JM. Pathology of aging B6;129 mice. *Toxicol Pathol.* 2001;29:653–661.
54. Black BJ Jr, McMahan CA, Masoro EJ, et al. Senescent terminal weight loss in the male F344 rat. *Am J Physiol Regul Integr Comp Physiol.* 2003;284:R336–R342.
55. Brigelius-Flohe R, Maurer S, Lotzer K, et al. Overexpression of PHGPx inhibits hydroperoxide-induced oxidation, NFkappaB activation and

apoptosis and affects oxLDL-mediated proliferation of rabbit aortic smooth muscle cells. *Atherosclerosis*. 2000;152:307–316.
56. Wang HP, Qian SY, Schafer FQ, et al. Phospholipid hydroperoxide glutathione peroxidase protects against singlet oxygen-induced cell damage of photodynamic therapy. *Free Radic Biol Med*. 2001;30: 825–835.
57. Hurst R, Korytowski W, Kriska T, et al. Hyperresistance to cholesterol hydroperoxide-induced peroxidative injury and apoptotic death in a tumor cell line that overexpresses glutathione peroxidase isotype-4. *Free Radic Biol Med*. 2001;31:1051–1065.
58. Petrosillo G, Ruggiero FM, Paradies G. Role of reactive oxygen species and cardiolipin in the release of cytochrome *c* from mitochondria. *FASEB J*. 2003;17:2202–2208.
59. Kriska T, Korytowski W, Girotti AW. Role of mitochondrial cardiolipin peroxidation in apoptotic photokilling of 5-amino-levulinate-treated tumor cells. *Arch Biochem Biophys*. 2005;433:435–446.
60. Warner HR. Apoptosis: a two-edged sword in aging. *Anticancer Res*. 1999;19:2837–2842.
61. Franceschi C. Cell proliferation, cell death and aging. *Aging*. 1989; 1:3–15.
62. Hughes J, Savill JS. Apoptosis in glomerulonephritis. *Curr Opin Nephrol Hypertens*. 2005;14:389–395.
63. Giorgio M, Migliaccio E, Orsini F, et al. Electron transfer between cytochrome *c* and p66Shc generates reactive oxygen species that trigger mitochondrial apoptosis. *Cell*. 2005;122:221–233.
64. Migliaccio E, Giorgio M, Pelicci PG. Apoptosis and aging: role of p66Shc redox protein. *Antioxid Redox Signal*. 2006;8:600–608.

Received May 1, 2007
Accepted June 19, 2007
Decision Editor: Huber R. Warner, PhD